

# Branching fractions of semileptonic $D$ and $D_s$ decays from the covariant light-front quark model

Hai-Yang Cheng and Xian-Wei Kang

*Institute of Physics, Academia Sinica, Taipei, Taiwan 115*

## Abstract

Based on the predictions of the relevant form factors from the covariant light-front quark model, we show the branching fractions for the  $D(D_s) \rightarrow (P, S, V, A) \ell \nu_\ell$  ( $\ell = e$  or  $\mu$ ) decays, where  $P$  denotes the pseudoscalar meson,  $S$  the scalar meson with a mass above 1 GeV,  $V$  the vector meson and  $A$  the axial-vector one. Comparison with the available experimental results are made, and we find an excellent agreement. The predictions for other decay modes can be tested in a charm factory, e.g., the BESIII detector. The future measurements will definitely further enrich our knowledge on the hadronic transition form factors as well as the inner structure of the even-parity mesons ( $S$  and  $A$ ).

## I. INTRODUCTION

The Cabibbo-Kobayashi-Maskawa (CKM) matrix describing the quark flavor mixing [1] has been a key skeleton of the Standard Model (SM). Precise determination of its matrix elements is one of the central tasks for both theoretical and experimental colleagues all along. Any deviation from the unitarity relation is believed to be an exciting signal of New Physics (NP). As it is known, the semileptonic decay of heavy flavor meson plays an important role in extracting CKM elements, e.g., the  $V_{cd}$  from  $c \rightarrow d$  decay and  $V_{cs}$  from  $c \rightarrow s$  decay. The extraction of  $V_{cq}$  ( $q = d$  or  $s$ ) needs some sophisticated knowledge of the form factors relevant for the decay process.

We first briefly introduce the form factors to be used in this work. Among the various models, we will concentrate on the description of form factors from the covariant light-front quark model (CLFQM). In 1949, Dirac proposed three different forms fulfilling the special theory of the relativity and the Hamiltonian formulation of the dynamics [2]: instant form, point form and light-front form. The light-front form ( $x^+ = x^0 + x^3 = 0$ ) has the advantages that there are only three Hamiltonians from the ten fundamental quantities in the Poincaré group and that the square root is absent in the Hamiltonians such that one can avoid the negative-energy states. The quark model expressed in the light-front form constitutes the so-called light-front quark model, which has been extensively developed to treat the electroweak (radiative and semileptonic) decays of the mesons in the early 1990s [3, 4]. In such theory, one can first draw the Feynmann diagram and then write down the amplitude. Meson is a bound state of its quark component  $q\bar{q}$ . The vertex function between the meson and its  $q\bar{q}$  is obtained from the wave function composed of the momentum distribution of the constituent quarks in the meson and the spin part. The latter involves the Melosh-type rotation from the conventional spin state (or the so-called instant form of the spin state by Dirac) to the one in the light-front form. In fact, the occurrence of the light-front form can be also easily seen from the infinite-momentum frame [5]. The quark internal line is just given by the fermion propagator. Taking the plus component of the corresponding current matrix element will give the final result for the form factor. Note that in such a conventional light-front quark model, the internal quarks are on their mass shells, and the zero-mode effect is missed which renders the theory non-covariant. Considering these defects, the covariant light-front quark model (CLFQM) [6] was later proposed (see also more works on this aspect in [7–9])

and a very recent work [10]). Following the lines of Ref. [6], Cheng, Chua and Hwang have systematically studied the decay constants and form factors for the  $S$ - and  $P$ -wave mesons in 2003 [11], while an update was done in Ref. [12]. In the latter reference, the author applied the available experimental information and the lattice results for the decay constants to constrain (part of) the parameters  $\beta$  in the wave functions, and also incorporated the  $D_s$  and  $B_s$  decays. However, only the relevant form factors are presented in Refs. [11, 12]. In this work we shall further provide the branching fractions which are the *true observables* in experiment such that we can make a *direct* comparison between theory and experiment. Moreover, the large statistics accumulated by the BESIII is capable of carrying out such a task.

We discuss below how we understand the main usage of the branching fractions predicted in this work. Our considerations are as follows:

- $|V_{cd}|$  and  $|V_{cs}|$  are well-determined quantities, which are also used as input for calculating the branching fractions.
- We will see below that the comparison of the theoretical predictions with experimental measurements for  $P$  and  $V$  mesons leads to an excellent agreement. This demonstrates that the CLFQM works very well.
- To calculate the branching fractions, we have considered the underlying structure of the final-state meson, e.g., the mixing angles for axial-vector  $f_1$ ,  $h_1$  and  $K_1$  mesons. Especially, the scalar isosinglet  $f_0$  states above 1 GeV are considered as the mixture of  $q\bar{q}$  and the glueball state  $G$ . The confrontation of our theoretical predictions with experiment will *help pin down the issue of the underlying structures of these mesons*. Emphasis will be put on the scalar and axial-vector mesons, which are less understood compared to the pseudoscalar and vector octet ones.
- The three-body semileptonic decay provides a clean environment for the study of the weak hadronic transition as well as the underlying structure of the involved mesons due to the absence of the final-state interactions (FSIs) between hadrons <sup>1</sup>.

---

<sup>1</sup> FSIs in the four-body semileptonic decay mode, e.g.  $D \rightarrow \pi\pi l\bar{\nu}_l$ , can be carefully explored following the line sketched in Ref. [13]

Experimentally, such a goal of testing the inner structure of the axial-vector and scalar mesons is doable due to the existing large statistics of  $D$  and  $D_s$  mesons. We need to point out that  $1.8 \times 10^7$   $D^0 \bar{D}^0$  and  $1.4 \times 10^7$   $D^+ D^-$  (at  $\psi(3770)$  peak),  $2.0 \times 10^7$   $D_s^+ D_s^-$  pairs (at the center of mass of 4.18 GeV) will be accumulated per year according to the design plan of BESIII [14–16]. For a super tau-charm factory, the luminosity will be further enhanced by 100 times [17, 18].

The outline of this work is as follows. For completeness, we show in Sec. II the formula for decay rates in details. Then in Sec. III the results for the branching fractions are summarized in Table I for the electron mode and II for the muon mode. The discussions are also presented there. Sec. IV comes to our conclusions.

## II. FORM FACTORS, DECAY RATES

We will follow the Bauer-Stech-Wirbel (BSW) model [19] for the convention of form factors and its extension to scalar and axial-vector mesons [11]. The pseudoscalar, scalar, vector, and axial-vector mesons are denoted by  $P$ ,  $S$ ,  $V$  and  $A$ , respectively. The form factors are given by <sup>2</sup>

$$\begin{aligned} \langle P(p'') | V_\mu | D_{(s)}(p') \rangle = & \left( p_\mu - \frac{m_{D_{(s)}}^2 - m_P^2}{q^2} q_\mu \right) F_1^{D_{(s)} \rightarrow P}(q^2) \\ & + \frac{m_{D_{(s)}}^2 - m_P^2}{q^2} q_\mu F_0^{D_{(s)} \rightarrow P}(q^2) \end{aligned} \quad (1)$$

for the transition of  $D_{(s)} \rightarrow P$ , and

$$\begin{aligned} \langle S(p'') | A_\mu | D_{(s)}(p') \rangle = & -i \left[ \left( p_\mu - \frac{m_{D_{(s)}}^2 - m_S^2}{q^2} q_\mu \right) F_1^{D_{(s)} \rightarrow S}(q^2) \right. \\ & \left. + \frac{m_{D_{(s)}}^2 - m_S^2}{q^2} q_\mu F_0^{D_{(s)} \rightarrow S}(q^2) \right]. \end{aligned} \quad (2)$$

for the  $D_{(s)} \rightarrow S$  transition. In above equations,  $V_\mu$  and  $A_\mu$  are the corresponding vector and axial-vector currents dominating the weak decay. The momenta  $p$  and  $q$  are defined as  $p = p' + p''$  and  $q = p' - p''$ , where  $p'(p'')$  is the four-momentum of the initial (final) meson. It has been shown [11, 21] that the additional factor of  $(-i)$  in Eq. (2) follows from the

---

<sup>2</sup> Some early studies on the flavor-symmetry breaking of  $D \rightarrow P$  form factors can be found in e.g., Ref. [20].

demand of positive form factors; it can be also seen by the calculations utilizing the heavy quark symmetry. As for the  $D_{(s)} \rightarrow V$  transition, we have

$$\langle V(p'', \epsilon''^*) | V_\mu | D_{(s)}(p') \rangle = -\frac{1}{m_{D_{(s)}} + m_V} \epsilon_{\mu\nu\alpha\beta} \epsilon''^{*\nu} p^\alpha q^\beta V(q^2), \quad (3)$$

$$\begin{aligned} \langle V(p'', \epsilon''^*) | A_\mu | D_{(s)}(p') \rangle = i \Bigg\{ & (m_{D_{(s)}} + m_V) \left[ \epsilon_\mu''^* - \frac{\epsilon''^* \cdot p}{q^2} q_\mu \right] A_1(q^2) \\ & - \frac{\epsilon''^* \cdot p}{m_{D_{(s)}} + m_V} \left[ p_\mu - \frac{m_{D_{(s)}}^2 - m_V^2}{q^2} q_\mu \right] A_2(q^2) \\ & + 2m_V \frac{\epsilon''^* \cdot p}{q^2} q_\mu A_0(q^2) \Bigg\} \end{aligned} \quad (4)$$

where the relation between  $A_3(q^2)$  and  $A_1(q^2), A_2(q^2)$  has been used. Finally, form factors for the  $D_{(s)} \rightarrow A$  transition read

$$\langle A(p'', \epsilon''^*) | A_\mu | D_{(s)}(p') \rangle = -\frac{1}{m_{D_{(s)}} - m_A} \epsilon_{\mu\nu\alpha\beta} \epsilon''^{*\nu} p^\alpha q^\beta A(q^2), \quad (5)$$

$$\begin{aligned} \langle A(p'', \epsilon''^*) | V_\mu | D_{(s)}(p') \rangle = -i \Bigg\{ & (m_{D_{(s)}} - m_A) \left[ \epsilon_\mu''^* - \frac{\epsilon''^* \cdot p}{q^2} q_\mu \right] V_1(q^2) \\ & - \frac{\epsilon''^* \cdot p}{m_{D_{(s)}} - m_A} \left[ p_\mu - \frac{m_{D_{(s)}}^2 - m_A^2}{q^2} q_\mu \right] V_2(q^2) \\ & + 2m_A \frac{\epsilon''^* \cdot p}{q^2} q_\mu V_0(q^2) \Bigg\}. \end{aligned} \quad (6)$$

Two remarks are in order:

- For the  $D_{(s)} \rightarrow A$  transition form factors, we follow the definitions in Refs. [11, 22], i.e., we have made the replacements  $m_{D_{(s)}} \pm m_A \longrightarrow m_{D_{(s)}} \mp m_A$  compared to the obsolete ones in Ref. [23] since it has been shown in [11] that such replacements will make the transitions  $B \rightarrow D_0^*, D_1$  fulfilling the similar heavy-quark-symmetry relations as that for  $B \rightarrow D, D^*$  ones.
- In order to cancel the singularity due to  $q^2 = 0$ , we need the constraints

$$\begin{aligned} F_1^{D_{(s)} \rightarrow S(P)}(0) &= F_0^{D_{(s)} \rightarrow S(P)}(0), \\ 2m_V A_0(0) &= (m_{D_{(s)}} + m_V) A_1(0) - (m_{D_{(s)}} - m_V) A_2(0), \\ 2m_A V_0(0) &= (m_{D_{(s)}} - m_A) V_1(0) - (m_{D_{(s)}} + m_A) V_2(0). \end{aligned} \quad (7)$$

It is easily checked that the corresponding values of form factors listed in Refs. [11, 12] indeed fulfill them.

As mentioned in the Introduction, Ref. [12] is an updated version of Ref. [11], and we will stick to the form factors obtained there based on CLFQM.

In CLFQM  $q^+ = 0$  is chosen, and then  $q^2 = -q_\perp^2 < 0$ , i.e., in the spacelike region. However, the physical situation requires form factors be timelike ( $q^2 > 0$ ). In Ref. [3], an explicit form for the form factor is proposed under the assumption that it is a continuously differentiable function of  $q^2$ . That form is assumed to be valid in the full range of  $q^2$ , i.e., the timelike region can be continued from the spacelike one, thus the values in the environment of  $q^2 = 0$  is crucial. The parameters appearing in the form factor are determined by the calculation of the appropriate derivatives. In fact, the parameters can be better determined by a fit, as has been done in Refs. [11, 12]. Explicitly, we take

$$F(q^2) = \frac{F(0)}{1 - a(q^2/m_D^2) + b(q^2/m_D^2)^2}, \quad (8)$$

where the values for  $F(0), a, b$  corresponding to the transitions considered in this work have been calculated in Refs. [11, 12]. As discussed in [11], the form factor  $V_2(q^2)$  for  $D_{(s)} \rightarrow A(1^{+-})$  transition approaches zero at very large  $-|q^2|$  where the three-parameter parametrization (2.19) becomes questionable. To overcome this difficulty, we will fit this form factor to the form

$$V_2(q^2) = \frac{V_2(0)}{(1 - q^2/m_D^2)[1 - a(q^2/m_D^2) + b(q^2/m_D^2)^2]}. \quad (9)$$

In Fig. 1, we illustrate the difference between Eqs. (8) and (9) for  $V_2(q^2)$  using the same values  $F(0) = -0.10$ ,  $a = 0.26$ ,  $b = 0.090$  for  $V_2^{D \rightarrow b_1}$  as in Table 9 of Ref. [12]. Clearly, the difference between the solid and dashed lines is large such that their integration over  $q^2$  (the area formed by the curve and  $x$ -axis) involved by the differential decay rate can differ by a factor of two. One may also consider whether  $m_D$  should be replaced by  $m_{D_s}$  when treating the  $D_s$  decays. In fact, the difference induced by such a replacement is negligible, as can be seen by comparing the dotted and solid lines or the dashed and dot-double-dashed lines in Fig. 1.

In terms of the form factors given above, the differential decay rate for  $D_{(s)} \rightarrow S(P)$  reads ( $\hat{m}_l^2 = m_l^2/q^2$ )

$$\frac{d\Gamma}{dq^2} = (1 - \hat{m}_l^2)^2 \frac{\sqrt{\lambda(m_{D(s)}^2, m_{S(P)}^2, q^2)} G_F^2 |V_{cq}|^2}{384 m_{D(s)}^3 \pi^3} \left[ (2 + \hat{m}_l^2) \lambda(m_{D(s)}^2, m_{S(P)}^2, q^2) [F_1^{D(s) \rightarrow S(P)}(q^2)]^2 \right]$$

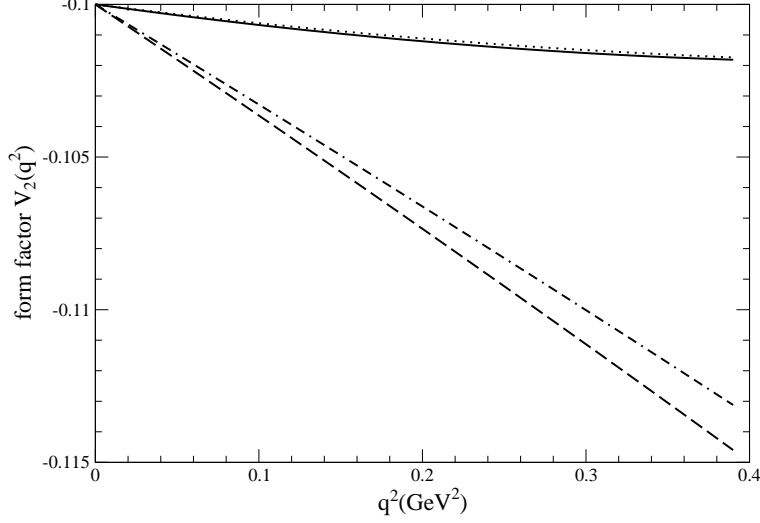


FIG. 1. Comparison of the different forms for the form factor  $V_2(q^2)$  corresponding to the values  $F(0) = -0.10$ ,  $a = 0.26$ ,  $b = 0.090$ . The solid (dashed) line corresponds to Eq. (8) (Eq. (9)), while the dotted (dot-double-dashed) line denotes Eq. (8) (Eq. (9)) with  $m_D$  replaced by  $m_{D_s}$ .

$$+3\hat{m}_l^2(m_{D(s)}^2 - m_{S(P)}^2)[F_0^{D(s) \rightarrow S(P)}(q^2)]^2 \Big] (10)$$

with the quark flavor  $q = s$  or  $d$ . The  $D_{(s)} \rightarrow A\ell\nu_\ell$  decay width has the expression

$$\frac{d\Gamma}{dq^2} = \frac{d\Gamma_L}{dq^2} + \frac{d\Gamma_+}{dq^2} + \frac{d\Gamma_-}{dq^2}, \quad (11)$$

with

$$\begin{aligned} \frac{d\Gamma_L}{dq^2} = (1 - \hat{m}_l^2)^2 \frac{\sqrt{\lambda(m_{D(s)}^2, m_A^2, q^2)} G_F^2 |V_{cq}|^2}{384 m_{D(s)}^3 \pi^3} \left\{ 3\hat{m}_l^2 \lambda(m_{D(s)}^2, m_A^2, q^2) [V_0(q^2)]^2 + \right. \\ \left. \frac{2 + \hat{m}_l^2}{4m_A^2} \left[ (m_{D(s)}^2 - m_A^2 - q^2)(m_{D(s)} - m_A) V_1(q^2) - \frac{\lambda(m_{D(s)}^2, m_A^2, q^2)}{m_{D(s)} - m_A} V_2(q^2) \right]^2 \right\}, \quad (12) \end{aligned}$$

$$\begin{aligned} \frac{d\Gamma_\pm}{dq^2} = (1 - \hat{m}_l^2)^2 \frac{\sqrt{\lambda(m_{D(s)}^2, m_A^2, q^2)} G_F^2 |V_{cq}|^2}{384 m_{D(s)}^3 \pi^3} \left\{ (m_l^2 + 2q^2) \lambda(m_{D(s)}^2, m_A^2, q^2) \right. \\ \left. \times \left[ \frac{A(q^2)}{m_{D(s)} - m_A} \mp \frac{(m_{D(s)} - m_A) V_1(q^2)}{\sqrt{\lambda(m_{D(s)}^2, m_A^2, q^2)}} \right]^2 \right\}. \quad (13) \end{aligned}$$

The  $D_{(s)} \rightarrow V\ell\nu_\ell$  decay rate can be obtained from Eqs. (12) and (13) by the following replacements:

$$\{A(q^2), V_0(q^2), V_1(q^2), V_2(q^2)\} \longrightarrow \{V(q^2), A_0(q^2), A_1(q^2), A_2(q^2)\},$$

$$\begin{aligned}
m_A &\longrightarrow m_V, \\
m_{D_{(s)}} \mp m_A &\longrightarrow m_{D_{(s)}} \pm m_V.
\end{aligned}
\tag{14}$$

Note that the form factors are real-valued. These expressions agree with Refs. [24–26] except for some obvious typos in Ref. [26].

### III. RESULTS AND DISCUSSION

In this section, we consider the semileptonic decays of both  $D$  and  $D_s$  mesons. For the final states, we consider the  $P, V, S, A$  ones summarized below:

- $P$  is the pseudoscalar Goldstone boson  $\pi, K, \eta, \eta'$ .
- $V$  is the vector octet containing  $\rho, \omega, K^*, \phi$ .
- $S$  is the scalar meson lying above 1 GeV, and refers to  $a_0(1450), f_0(1500), f_0(1710)$  and  $K_0^*(1450)$ . The state  $f_0(1370)$  will not be considered by us since its mass and width have not been well determined yet. PDG [27] shows that its pole position is at  $(1200 - 1500) - i(150 - 250)$  MeV, and the Breit-Wigner or  $K$ -matrix mass and width at  $(1200 - 1500) - i(200 - 500)$  MeV. Note that the imaginary part of the pole position corresponds to half of the width. From this prospective, the main emphasis should be first concentrated on its pole determination. Otherwise, the branching fraction cannot be predicted in a comparable precision as other  $S$  states. Concerning the various experimental issues about the  $S$  states above 1 GeV, one may refer to the review [28].
- The axial-vector meson denoted by  $A$  with the spin and parity quantum numbers  $J^P = 1^-$  is classified into two categories:  $1^{++}$  and  $1^{+-}$ . The former contains  $a_1(1260), f_1(1285), f_1(1420)$  while the latter consists of  $b_1(1235), h_1(1170)$  and  $h_1(1380)$ . We will not consider  $a_1(1260)$  due to its extremely broad width 200 – 600 MeV [27]. We also note that  $a_1(1260)$  and  $b_1(1235)$  cannot be mixed together due to the opposite charge conjugation parity ( $C$ -parity). In fact, for the fermion-antifermion pair, one has  $C = (-1)^{L+S}$  with  $L$  and  $S$  denoting the orbital angular momentum and total spin between the fermion-antifermion system. But  $K_{1A}$  and  $K_{1B}$  do mix together to form the physical mass eigenstates  $K_1(1270)$  and  $K_1(1400)$  due to the strange and non-strange quark mass difference.

The properties of the pseudoscalar mesons  $\pi$ ,  $K$ ,  $\eta$  and the vector states  $\rho$ ,  $\omega$ ,  $\phi$ ,  $K^*$  are very well-known. The  $\eta$  and  $\eta'$  mixing can be written in terms of their quark states  $\eta_q$  and  $\eta_s$  corresponding to the  $q\bar{q} \equiv (u\bar{u} + d\bar{d})/\sqrt{2}$  and  $s\bar{s}$  components, respectively:

$$\begin{aligned}\eta &= \eta_q \cos \phi - \eta_s \sin \phi, \\ \eta' &= \eta_q \sin \phi + \eta_s \cos \phi,\end{aligned}\tag{15}$$

with the mixing angle  $\phi = 39.3^\circ \pm 1.0^\circ$  [29–31].

We now introduce the mixing scheme for axial-vector states as well as the scalar  $f_0$  states above 1 GeV. For the axial-vector mesons, we have [32]

$$\begin{aligned}f_1(1285) &= f_{1q} \sin \alpha_{f1} + f_{1s} \cos \alpha_{f1}, \\ f_1(1420) &= f_{1q} \cos \alpha_{f1} - f_{1s} \sin \alpha_{f1},\end{aligned}\tag{16}$$

with  $\alpha_{f1} = 69.7^\circ$ , and

$$\begin{aligned}h_1(1170) &= h_{1q} \sin \alpha_{h1} + h_{1s} \cos \alpha_{h1}, \\ h_1(1380) &= h_{1q} \cos \alpha_{h1} - h_{1s} \sin \alpha_{h1},\end{aligned}\tag{17}$$

with  $\alpha_{h1} = 86.7^\circ$ . As before,  $f_{1q}$  and  $h_{1q}$  denote the  $q\bar{q}$  component of  $f_1$  and  $h_1$ , respectively, while  $f_{1s}$  and  $h_{1s}$  denote the corresponding  $s\bar{s}$  components. Note that in the literature, the mixing angle  $\theta$  is often referred to the singlet-octet one, and  $\alpha = \theta + 54.7^\circ$  [33]. An “ideal” mixing is defined as  $\tan \theta = 1/\sqrt{2}$ , i.e.,  $\theta = 35.3^\circ$ . Clearly, the  $h_1(1170)$  is dominated by  $h_{1q}$ , while the  $h_1(1380)$  mainly consists of  $s\bar{s}$ . The mixing is described at the level of state and thus the amplitude  $\mathcal{A}$  (or the corresponding form factor) also obeys the relations

$$\begin{aligned}\mathcal{A}^{D \rightarrow f_1(1285)} &= \frac{1}{\sqrt{2}} \sin \alpha_{f1} \mathcal{A}^{D \rightarrow f_{1q}}, & \mathcal{A}^{D_s \rightarrow f_1(1285)} &= \cos \alpha_{f1} \mathcal{A}^{D_s \rightarrow f_{1s}}, \\ \mathcal{A}^{D \rightarrow f_1(1420)} &= \frac{1}{\sqrt{2}} \cos \alpha_{f1} \mathcal{A}^{D \rightarrow f_{1q}}, & \mathcal{A}^{D_s \rightarrow f_1(1420)} &= -\sin \alpha_{f1} \mathcal{A}^{D_s \rightarrow f_{1s}}.\end{aligned}\tag{18}$$

Note that there are no  $D \rightarrow f_{1s}$  and  $D_s \rightarrow f_{1q}$  transitions. The factor of  $1/\sqrt{2}$  coming from  $(u\bar{u} + d\bar{d})/\sqrt{2}$  should be kept in mind since only the  $d\bar{d}$  component of  $f_1$  state is used in the  $D \rightarrow f_1$  transition. Similar relations also hold for  $h_1$ , and  $f_0$  states below

$$\begin{aligned}\mathcal{A}^{D \rightarrow f_0(1370)} &= 0.78/\sqrt{2} \mathcal{A}^{D \rightarrow f_{0q}}, \\ \mathcal{A}^{D \rightarrow f_0(1500)} &= -0.54/\sqrt{2} \mathcal{A}^{D \rightarrow f_{0q}}, \\ \mathcal{A}^{D \rightarrow f_0(1710)} &= 0.32/\sqrt{2} \mathcal{A}^{D \rightarrow f_{0q}},\end{aligned}$$

$$\begin{aligned}
\mathcal{A}^{D_s \rightarrow f_0(1370)} &= 0.51 \mathcal{A}^{D_s \rightarrow f_{0s}}, \\
\mathcal{A}^{D_s \rightarrow f_0(1500)} &= 0.84 \mathcal{A}^{D_s \rightarrow f_{0s}}, \\
\mathcal{A}^{D_s \rightarrow f_0(1710)} &= 0.18 \mathcal{A}^{D_s \rightarrow f_{0s}}.
\end{aligned} \tag{19}$$

The physical mass eigenstates  $K_1(1270)$  and  $K_1(1400)$  are the mixture of the  $^1P_1$  state  $K_{1B}$  and  $^3P_1$  state  $K_{1A}$  [33],

$$\begin{aligned}
K_1(1270) &= K_{1A} \sin \theta_{K_1} + K_{1B} \cos \theta_{K_1}, \\
K_1(1400) &= K_{1A} \cos \theta_{K_1} - K_{1B} \sin \theta_{K_1},
\end{aligned} \tag{20}$$

and we will take  $\theta_{K_1} = 33^\circ$  from the analysis of Ref. [32]. The corresponding form factors can be obtained by

$$\begin{aligned}
\mathcal{F}^{D_{(s)} \rightarrow K_1(1270)}(q^2) &= \mathcal{F}^{D_{(s)} \rightarrow K_{1A}}(q^2) \sin \theta_{K_1} + \mathcal{F}^{D_{(s)} \rightarrow K_{1B}}(q^2) \cos \theta_{K_1}, \\
\mathcal{F}^{D_{(s)} \rightarrow K_1(1400)}(q^2) &= \mathcal{F}^{D_{(s)} \rightarrow K_{1A}}(q^2) \cos \theta_{K_1} - \mathcal{F}^{D_{(s)} \rightarrow K_{1B}}(q^2) \sin \theta_{K_1},
\end{aligned} \tag{21}$$

with  $\mathcal{F}$  denoting  $V(q^2)$ ,  $A_0(q^2)$ ,  $A_1(q^2)$ ,  $A_2(q^2)$ .

Concerning the scalar nonet with mass above 1 GeV, the  $a_0(1450)$  and  $K_0^*(1430)$  are believed to be the conventional  $q\bar{q}$  mesons, while the interpretations of  $f_0(1370)$ ,  $f_0(1500)$  and  $f_0(1710)$  are not yet achieved in full agreement, although it is generally argued that one of them contains mainly the scalar glueball. The controversial issue is focused on which one is primarily a glueball. The analysis of Ref. [34] shows that the  $f_0(1710)$  should have a large glueball component and  $f_0(1500)$  is mainly a flavor octet:

$$\begin{pmatrix} f_0(1370) \\ f_0(1500) \\ f_0(1710) \end{pmatrix} = \begin{pmatrix} 0.78(2) & 0.52(3) & -0.36(1) \\ -0.55(3) & 0.84(2) & 0.03(2) \\ 0.31(1) & 0.17(1) & 0.934(4) \end{pmatrix} \begin{pmatrix} f_{0q} \\ f_{0s} \\ G \end{pmatrix} \tag{22}$$

with  $G$  denoting a glueball. More interesting discussions on the details can be found in Ref. [34] in which all the existing lattice calculations and experimental data have been considered. Hence, we adopt the mixing scheme given in Eq. (22). In fact, we wish to stress that the proposed measurements of semileptonic  $D$  or  $D_s$  transitions to  $f_0$  states will be a powerful test for its inner structure due to the absence of the final-state interaction between  $f_0$  and the lepton pair. At least, it can serve as a useful complement.

Based on the expressions in Sec. II and the information for the form factors in Ref. [12], one can deduce the decay rates  $d\Gamma/dq^2$  for  $D_{(s)} \rightarrow M\ell^+\nu_\ell$  decay and the branching fraction

as

$$\mathcal{B} = \frac{1}{\Gamma_{D(s)}} \int_{m_\ell^2}^{(m_{D(s)} - m_M)^2} \frac{d\Gamma}{dq^2}. \quad (23)$$

We refrain from repeating the values shown in Ref. [12], where the form factors for  $D_{(s)}$  decays to  $P, V, S, A(1^{++}), A(1^{+-})$  can be found in Tables 4–9, respectively. Our results for the branching fractions are summarized in Table I for the electron decay mode and Table II for the muon mode. Strictly speaking, the  $D$  decays corresponds to the charged case, since in the CLFQM the decay constant for  $D^+$  is used to determine the  $\beta$  in the vertex function [11, 12].

Several remarks are in order:

- For  $D_{(s)} \rightarrow (P, V)e^+\nu_e$  decay, there are abundant experimental data. The most recent measurements for the  $D_s$  decay were done by BESIII [35] and by Hietala et al. based on the CLEO data [36]. Our results are in excellent agreement with them within errors. Especially for  $D \rightarrow \pi, D \rightarrow \eta, D_s \rightarrow \eta, D \rightarrow \rho, D_s \rightarrow K^*$ , the central values even match the experimental numbers exactly. Such a surprisingly good agreement is beyond our expectation as *a priori* the CLFQM does not “know” anything about these experimental information. In other words, these values of the branching fractions can be regarded as the predictions of CLFQM as all the input parameters (quark masses,  $\beta$  values in the vertex function) are not fitted by the information of the measured rates. This in turn demonstrates its predictive power. After all, we wish to stress again that an extrapolation from the space-like region to the physical time-like one with the pole-model behavior (Eq. (8)) has been utilized for form factors.
- According to the BESIII plan [14–16],  $1.8 \times 10^7 D^0 \bar{D}^0$ ,  $1.4 \times 10^7 D^+ D^-$ ,  $2.0 \times 10^7 D_s^+ D_s^-$  pairs will be accumulated per year. The decays  $D_s^+ \rightarrow h_1(1380), K_1(1270)$  will be easily measured and tested. But the decays involving  $f_0(1710)$  as a final state cannot be detected currently due to the limited statistics. However, for a super tau-charm factory, the luminosity will be enhanced by 100 times [17, 18, 37, 38], and then the goal for the measurement of these channels can be realized. We also note that CLEO has measured the branching fraction of  $D^0 \rightarrow K_1^-(1270)e^+\bar{\nu}_e$  with the result of  $(7.6 \pm 4.1) \times 10^{-4}$  [39]. Considering the lifetime difference between  $D^0$  and  $D^+$ , our result agrees with experiment.

- The origin for different orders of magnitudes for branching fractions is typically understood in terms of the Cabibbo suppression and/or phase space suppression (e.g., comparing  $D \rightarrow f_0(1500)$  and  $D \rightarrow f_0(1710)$ ).
- The predicted central values of the branching fractions for  $D \rightarrow \omega, D \rightarrow \bar{K}, D \rightarrow \bar{K}^*, D_s \rightarrow \phi$  semileptonic decays are in reasonable agreement with the experimental measurements, but not as excellent as the ones for  $D \rightarrow \pi, D \rightarrow \rho, D_s \rightarrow \eta, D_s \rightarrow K^*$  as exhibited in Table I. In particular, the difference for the  $D \rightarrow \bar{K}^*$  case is a bit larger, a factor of 1.4 between theory and experiment comparing the central values. This reminds us of some possible theoretical errors. The main uncertainties come from form factors, the CKM matrix elements  $|V_{cs}|$  and  $|V_{cd}|$ , and also the mixing angles (e.g., Eqs. (16), (17) and (22)). In Ref. [12], the uncertainty of decay constants has been propagated to the values of  $\beta$  in light-cone wave functions, otherwise, a 10% variation in  $\beta$  is allowed. The uncertainty arising from the form factors is typically of the order of 2%. The CKM matrix elements

$$|V_{cs}| = 0.995 \pm 0.016, \quad |V_{cd}| = 0.220 \pm 0.005, \quad (24)$$

are quoted by PDG [27]. Considering the modulus squared, this will yield around 5% uncertainty. The uncertainty induced by the mixing angle needs more care. We assign the uncertainties of  $8^\circ, 6^\circ, 4^\circ$  to  $\alpha_{f_1}, \alpha_{h_1}, \theta_{K_1}$ , respectively, guided by Ref. [32]. Allowing those variations, we get (rough) error estimate. When the uncertainty is comparably large as the central value, we show the resulting minimum and maximum in the brackets. For example, the mixing angle for  $h_1(1170)$  and  $h_1(1380)$  states ( $\alpha_{h_1}$ ) can cross  $90^\circ$ , where the transitions  $D \rightarrow h_1(1170)$  and  $D_s \rightarrow h_1(1380)$  are allowed, but not  $D_s \rightarrow h_1(1170)$  and  $D \rightarrow h_1(1380)$ . This shows the origin of vanishing branching fractions of  $D_s \rightarrow h_1(1170)\ell\nu_\ell$  and  $D \rightarrow h_1(1380)\ell\nu_\ell$  in Tables I and II. Indeed, the uncertainty in the mixing angles dominates the error estimate for  $D \rightarrow A$  transitions. From this point of view, it should be understood that the BESIII measurement on these channels will be highly meaningful for a “precise” determination of the mixing angle, as also mentioned in the Introduction.

- We also comment on the semileptonic decay mode involving a tau lepton. We have the masses [27]  $M(D) = 1869.59 \pm 0.09$  MeV,  $M(D_s) = 1968.28 \pm 0.10$  MeV, and

$M(\tau) = 1776.86 \pm 0.12$  MeV. Hence, only the decay  $D \rightarrow \tau \nu_\tau$  is allowed by phase space, which is constrained to be smaller than  $1.2 \times 10^{-3}$  with the confidence level of 90%. When it comes to  $D_s$  decays to  $\tau$  mode,  $D_s^+ \rightarrow \pi^0 \tau^+ \nu_\tau$  is also allowed besides  $D_s^+ \rightarrow \tau^+ \nu_\tau$ . However, the aforementioned semileptonic tau mode will be highly suppressed since there is no valence  $s$  quark in the pion. One possible mechanism will be the process  $D_s^+ \rightarrow \eta \tau^+ \nu_\tau \rightarrow \pi^0 \tau^+ \nu_\tau$  via the  $\eta - \pi^0$  mixing.

We wish to comment that even-parity light mesons, including the axial-vector meson, and the scalar meson above 1 GeV can be also studied via  $D_{(s)}$  two-body decays [40, 41] within the framework of the topological diagram approach and the factorization scheme. The semileptonic decay modes investigated here will provide a more clean environment to explore the nature of these mesons owing to the absence of the strong hadronic final-state interactions manifested in the two-body hadronic decay. Furthermore, the size of the branching fractions considered here is of the same order as the ones in Refs.[40, 41] typically ranging from  $10^{-6}$  to  $10^{-3}$ . So, at least, our proposal for the semileptonic mode can be done as a supplement.

At last, we comment on the light scalars close to or below 1 GeV, namely the  $a_0(980)$ ,  $f_0(980)$  and  $f_0(500)$  mesons. The structure of these mesons are still controversial to date. One of the popular viewpoints is to regard them as the tetraquarks (see e.g., Ref. [42]) or the molecular states of  $\pi\pi$  and  $K\bar{K}$  (see also a very recent work [43]), since the conventional  $q\bar{q}$  assignment will encounter some severe problems contradicting with experiment, see the discussions in Refs. [41, 44]. A complete list of references can be found in the reviews [45, 46]. If they are indeed tetraquark states, it will be difficult to tackle them by the CLFQM which is only suitable for treating the  $q\bar{q}$  meson. However, the attempt of probing  $f_0(500)$  and  $f_0(980)$  using the CLFQM by assigning them as the  $q\bar{q}$  configuration is available in Ref. [47], where the  $q\bar{q}$  and  $s\bar{s}$  mixing angle was obtained and the  $D^+ \rightarrow f_0(980)e^+\nu_e$  branching fraction was predicted. The underlying relations between the relevant form factors are similar to those discussed above. Following the guidance of the values presented in Ref. [11], the shape parameter  $\beta$  was (somewhat arbitrarily) chosen to be 0.30 allowing 10% variation there. That is, it is not fixed by the corresponding decay constant of the  $f_0(980)$  which is zero. The vanishing decay constants of the neutral  $f_0(500)$ ,  $a_0(980)$ ,  $f_0(980)$  are the consequence of the charge-conjugate invariance [11]. In other words, the shape parameter cannot be well fixed by the information of the decay constant, and instead, other model calculations may

be used.

Channel	$D \rightarrow \pi$	$D \rightarrow \bar{K}$	$D \rightarrow \eta$	$D \rightarrow \eta'$	$D_s \rightarrow K$	$D_s \rightarrow \eta$	$D_s \rightarrow \eta'$
Theory ( $10^{-2}$ )	$0.41 \pm 0.03$	$10.32 \pm 0.93$	$0.12 \pm 0.01$	$0.018 \pm 0.002$	$0.27 \pm 0.02$	$2.26 \pm 0.21$	$0.89 \pm 0.09$
PDG ( $10^{-2}$ )	$0.41 \pm 0.02$	$8.82 \pm 0.13$	$0.11 \pm 0.01$	$0.022 \pm 0.005$	$0.39 \pm 0.09$	$2.29 \pm 0.19$	$0.74 \pm 0.14$
Channel	$D \rightarrow \rho$	$D \rightarrow \omega$	$D \rightarrow \bar{K}^*$	$D_s \rightarrow K^*$	$D_s \rightarrow \phi$		
Theory ( $10^{-2}$ )	$0.23 \pm 0.02$	$0.21 \pm 0.02$	$7.5 \pm 0.7$	$0.19 \pm 0.02$	$3.1 \pm 0.3$		
PDG ( $10^{-2}$ )	$0.22^{+0.02}_{-0.03}$	$0.17 \pm 0.01$	$5.40 \pm 0.10$	$0.18 \pm 0.04$	$2.39 \pm 0.23$		
Channel	$D \rightarrow a_0(1450)$	$D \rightarrow f_0(1500)$	$D \rightarrow f_0(1710)$	$D \rightarrow K_0^*(1450)$	$D_s \rightarrow K_0^*(1450)$	$D_s \rightarrow f_0(1500)$	$D_s \rightarrow f_0(1710)$
Theory ( $10^{-5}$ )	$0.54 \pm 0.05$	$0.11 \pm 0.02$	$(4.7 \pm 0.8) \cdot 10^{-4}$	$29 \pm 3$	$2.7 \pm 0.2$	$15 \pm 3$	$0.034 \pm 0.006$
Channel	$D \rightarrow f_1(1285)$	$D \rightarrow f_1(1420)$	$D \rightarrow b_1(1235)$	$D \rightarrow h_1(1170)$	$D \rightarrow h_1(1380)$	$D_s \rightarrow h_1(1170)$	$D_s \rightarrow h_1(1380)$
Theory ( $10^{-5}$ )	$3.7 \pm 0.8$	$\{0.02, 0.14\}$	$7.4 \pm 0.7$	$14 \pm 1.5$	$\{0, 0.02\}$	$\{0, 19.7\}$	$64 \pm 7$
Channel	$D \rightarrow K_1(1270)$	$D \rightarrow K_1(1400)$	$D_s \rightarrow K_1(1270)$	$D_s \rightarrow K_1(1400)$	$D_s \rightarrow f_1(1285)$	$D_s \rightarrow f_1(1420)$	
Theory ( $10^{-5}$ )	$320 \pm 40$	$\{0.5, 2.0\}$	$17 \pm 2$	$\{0.05, 0.14\}$	$\{6.0, 36\}$	$25 \pm 5$	

TABLE I. Branching fractions of  $D^+$  and  $D_s^+$  decays to  $(P, V, S, A)e^+\nu_e$ . Units are shown in parentheses. PDG average values are taken from Ref. [27], while data are not yet available for the  $S$  and  $A$  modes. When the error bar is comparable to the central value, instead we show the minimum and maximum values in the brackets.

Channel	$D \rightarrow \pi$	$D \rightarrow \bar{K}$	$D \rightarrow \eta$	$D \rightarrow \eta'$	$D_s \rightarrow K$	$D_s \rightarrow \eta$	$D_s \rightarrow \eta'$
Theory ( $10^{-2}$ )	$0.41 \pm 0.03$	$10.07 \pm 0.91$	$0.12 \pm 0.01$	$0.017 \pm 0.002$	$0.26 \pm 0.02$	$2.22 \pm 0.20$	$0.85 \pm 0.08$
PDG ( $10^{-2}$ )		$8.74 \pm 0.19$					
Channel	$D \rightarrow \rho$	$D \rightarrow \omega$	$D \rightarrow \bar{K}^*$	$D_s \rightarrow K^*$	$D_s \rightarrow \phi$		
Theory ( $10^{-2}$ )	$0.22 \pm 0.02$	$0.20 \pm 0.02$	$7.0 \pm 0.7$	$0.19 \pm 0.02$	$2.9 \pm 0.3$		
PDG ( $10^{-2}$ )			$5.25 \pm 0.15$				
Channel	$D \rightarrow a_0(1450)$	$D \rightarrow f_0(1500)$	$D \rightarrow f_0(1710)$	$D \rightarrow K_0^*(1450)$	$D_s \rightarrow K_0^*(1450)$	$D_s \rightarrow f_0(1500)$	$D_s \rightarrow f_0(1710)$
Theory ( $10^{-5}$ )	$0.38 \pm 0.03$	$0.07 \pm 0.01$	$(2.5 \pm 0.4) \cdot 10^{-5}$	$22 \pm 2.0$	$2.2 \pm 0.2$	$12 \pm 2$	$0.014 \pm 0.002$
Channel	$D \rightarrow f_1(1285)$	$D \rightarrow f_1(1420)$	$D \rightarrow b_1(1235)$	$D \rightarrow h_1(1170)$	$D \rightarrow h_1(1380)$	$D_s \rightarrow h_1(1170)$	$D_s \rightarrow h_1(1380)$
Theory ( $10^{-5}$ )	$3.2 \pm 0.6$	$\{0.02, 0.12\}$	$6.4 \pm 0.6$	$12.2 \pm 1.3$	$\{0, 0.02\}$	$\{0, 17.4\}$	$54 \pm 6$
Channel	$D \rightarrow K_1(1270)$	$D \rightarrow K_1(1400)$	$D_s \rightarrow K_1(1270)$	$D_s \rightarrow K_1(1400)$	$D_s \rightarrow f_1(1285)$	$D_s \rightarrow f_1(1420)$	
Theory ( $10^{-5}$ )	$260 \pm 30$	$\{0.4, 1.7\}$	$15 \pm 2$	$\{0.05, 0.12\}$	$\{5.2, 30.6\}$	$21 \pm 5$	

TABLE II. Same as Table I but for the muon mode, i.e.,  $D^+$  and  $D_s^+$  decays to  $(P, V, S, A)\mu^+\nu_\mu$ .

## IV. CONCLUSION

The covariant light-front model is a powerful tool to predict the electroweak decay form factors. In Ref. [11], the authors have systematically calculated the form factors for  $D$  transition to  $S$ - and  $P$ -wave mesons. The extension to the  $D_s^+$  decay has been done in

Ref. [12], where the parameters  $\beta$  in the light-front wave functions were constrained by the available experimental information as well as the lattice results. Based on the form factors there, we have calculated the branching fractions for various channels of the  $D$  and  $D_s$  decays to  $(P, S, V, A) \ell \bar{\nu}_\ell$ , with  $P, S, V, A$  denoting a pseudoscalar, scalar above 1 GeV, vector and axial-vector, respectively, and  $\ell = e$  or  $\mu$ . Results are shown in Table I for the electron decay mode and Table II for the muon mode. Comparing to the available experimental data, we find the covariant light-front model works very well. The branching fractions for other channels are also predicted. The semileptonic decay mode provides a clean environment to examine the hadron structures. The experimental searches are pointed out. Most of them can be measured by the BESIII Collaboration, while for a future super tau-charm factory, the statistics will be enhanced by 100 times. These future measurements confronting with the theoretical predictions here will definitely shed light on our basic understanding of the semileptonic  $D$  and  $D_s$  decay as well as the inner structure of the relevant scalars with masses above 1 GeV and axial-vector mesons. Other approaches for probing the structures of the scalar and axial-vectors are compared and commented.

**Acknowledgments:** XWK is grateful to Hong-Wei Ke, Wei Wang, Hsiang-Nan Li for useful discussions and Hai-Bo Li for the insightful discussions on the BES measurements. He also specially acknowledges R. C. Verma for the clarification of Ref. [12]. This work is supported by the Ministry of Science and Technology of R.O.C. under Grant No. 104-2112-M-001-022.

- 
- [1] N. Cabibbo, Phys. Rev. Lett. **10**, 531 (1963). doi:10.1103/PhysRevLett.10.531; M. Kobayashi and T. Maskawa, Prog. Theor. Phys. **49**, 652 (1973). doi:10.1143/PTP.49.652
  - [2] P. A. M. Dirac, Rev. Mod. Phys. **21**, 392 (1949). doi:10.1103/RevModPhys.21.392
  - [3] W. Jaus, Phys. Rev. D **41**, 3394 (1990). doi:10.1103/PhysRevD.41.3394
  - [4] W. Jaus, Phys. Rev. D **44**, 2851 (1991). doi:10.1103/PhysRevD.44.2851
  - [5] M. Beyer, C. Kuhrtz and H. J. Weber, Annals Phys. **269**, 129 (1998) doi:10.1006/aphy.1998.5837 [nucl-th/9804021].
  - [6] W. Jaus, Phys. Rev. D **60**, 054026 (1999). doi:10.1103/PhysRevD.60.054026

- [7] H. M. Choi and C. R. Ji, Phys. Rev. D **89**, no. 3, 033011 (2014) doi:10.1103/PhysRevD.89.033011
- [8] H. M. Choi and C. R. Ji, Few Body Syst. **54**, 1633 (2013) doi:10.1007/s00601-012-0535-7 [arXiv:1212.6590 [hep-ph]].
- [9] H. M. Choi and C. R. Ji, Phys. Rev. D **58**, 071901 (1998) doi:10.1103/PhysRevD.58.071901 [hep-ph/9805438].
- [10] K. Chen, X. Liu and T. Matsuki, arXiv:1707.02523 [hep-ph].
- [11] H. Y. Cheng, C. K. Chua and C. W. Hwang, Phys. Rev. D **69**, 074025 (2004) doi:10.1103/PhysRevD.69.074025 [hep-ph/0310359].
- [12] R. C. Verma, J. Phys. G **39**, 025005 (2012) doi:10.1088/0954-3899/39/2/025005 [arXiv:1103.2973 [hep-ph]].
- [13] X. W. Kang, B. Kubis, C. Hanhart and U. G. Meißner, Phys. Rev. D **89**, 053015 (2014) doi:10.1103/PhysRevD.89.053015 [arXiv:1312.1193 [hep-ph]].
- [14] M. Ablikim *et al.* [BESIII Collaboration], Nucl. Instrum. Meth. A **614**, 345 (2010) doi:10.1016/j.nima.2009.12.050 [arXiv:0911.4960 [physics.ins-det]]
- [15] D. M. Asner *et al.*, Int. J. Mod. Phys. A **24**, S1 (2009) [arXiv:0809.1869 [hep-ex]].
- [16] H. B. Li, Front. Phys. (Beijing) **12**, no. 5, 121301 (2017) doi:10.1007/s11467-017-0691-9 [arXiv:1612.01775 [hep-ex]].
- [17] D. M. Asner, Frascati Phys. Ser. **41**, 377 (2006) [hep-ex/0605040].
- [18] A. E. Bondar *et al.* [Charm-Tau Factory Collaboration], Phys. Atom. Nucl. **76**, 1072 (2013) [Yad. Fiz. **76**, no. 9, 1132 (2013)]. doi:10.1134/S1063778813090032
- [19] M. Wirbel, B. Stech and M. Bauer, Z. Phys. C **29**, 637 (1985); M. Bauer, B. Stech, and M. Wirbel, *ibid*, **42**, 671 (1989).
- [20] M. Y. Khlopov, Sov. J. Nucl. Phys. **28**, 583 (1978) [Yad. Fiz. **28**, 1134 (1978)]; S. S. Gershtein and M. Y. Khlopov, JETP Lett. **23**, 338 (1976).
- [21] H. Y. Cheng and C. W. Chiang, Phys. Rev. D **81**, 074031 (2010) doi:10.1103/PhysRevD.81.074031 [arXiv:1002.2466 [hep-ph]].
- [22] H. Y. Cheng and C. K. Chua, Phys. Rev. D **74**, 034020 (2006) doi:10.1103/PhysRevD.74.034020 [hep-ph/0605073].
- [23] H. Y. Cheng, Phys. Rev. D **68**, 094005 (2003) doi:10.1103/PhysRevD.68.094005 [hep-ph/0307168].

- [24] H. Xu, Q. Huang, H. W. Ke and X. Liu, Phys. Rev. D **90**, no. 9, 094017 (2014) doi:10.1103/PhysRevD.90.094017 [arXiv:1406.5796 [hep-ph]].
- [25] L. Riggio, G. Salerno and S. Simula, arXiv:1706.03657 [hep-lat].
- [26] Y. J. Shi, W. Wang and Z. X. Zhao, Eur. Phys. J. C **76**, no. 10, 555 (2016) doi:10.1140/epjc/s10052-016-4405-1 [arXiv:1607.00622 [hep-ph]].
- [27] C. Patrignani et al. (Particle Data Group), Chin. Phys. C, **40**, 100001 (2016) and 2017 update.
- [28] E. Klempt and A. Zaitsev, Phys. Rept. **454**, 1 (2007) doi:10.1016/j.physrep.2007.07.006 [arXiv:0708.4016 [hep-ph]].
- [29] T. Feldmann, P. Kroll and B. Stech, Phys. Rev. D **58**, 114006 (1998) doi:10.1103/PhysRevD.58.114006 [hep-ph/9802409].
- [30] T. Feldmann, P. Kroll and B. Stech, Phys. Lett. B **449**, 339 (1999) doi:10.1016/S0370-2693(99)00085-4 [hep-ph/9812269].
- [31] T. Feldmann, Int. J. Mod. Phys. A **15**, 159 (2000) doi:10.1142/S0217751X00000082 [hep-ph/9907491].
- [32] H. Y. Cheng, Phys. Lett. B **707**, 116 (2012) doi:10.1016/j.physletb.2011.12.013 [arXiv:1110.2249 [hep-ph]];  
H. Y. Cheng, PoS Hadron **2013**, 090 (2013) [arXiv:1311.2370 [hep-ph]].
- [33] The Review “Quark model” in Ref. [27].
- [34] H. Y. Cheng, C. K. Chua and K. F. Liu, Phys. Rev. D **92**, no. 9, 094006 (2015) doi:10.1103/PhysRevD.92.094006 [arXiv:1503.06827 [hep-ph]]; Phys. Rev. D **74**, 094005 (2006) doi:10.1103/PhysRevD.74.094005 [hep-ph/0607206].
- [35] M. Ablikim *et al.* [BESIII Collaboration], Phys. Rev. D **94**, no. 11, 112003 (2016) doi:10.1103/PhysRevD.94.112003 [arXiv:1608.06484 [hep-ex]].
- [36] J. Hietala, D. Cronin-Hennessy, T. Pedlar and I. Shipsey, Phys. Rev. D **92** (2015) no.1, 012009 doi:10.1103/PhysRevD.92.012009 [arXiv:1505.04205 [hep-ex]].
- [37] Z. Zhou, Q. Luo, L. Wang, W. Xu and B. Zhang, Preliminary Concept and Key Technologies of HIEPA Accelerator, talk at the 7th International Particle Accelerator Conference (IPAC 2016) 08-13 May, 2016, Busan, Korea.
- [38] A. J. Bevan, Front. Phys. (Beijing) **11**, no. 1, 111401 (2016) doi:10.1007/s11467-015-0481-1 [arXiv:1508.00222 [hep-ex]].

- [39] M. Artuso *et al.* [CLEO Collaboration], Phys. Rev. Lett. **99**, 191801 (2007) [arXiv:0705.4276 [hep-ex]].
- [40] H. Y. Cheng, Phys. Rev. D **67**, 094007 (2003) doi:10.1103/PhysRevD.67.094007 [hep-ph/0301198].
- [41] H. Y. Cheng and C. W. Chiang, Phys. Rev. D **81**, 074031 (2010) doi:10.1103/PhysRevD.81.074031 [arXiv:1002.2466 [hep-ph]].
- [42] N. N. Achasov and A. V. Kiselev, Phys. Rev. D **86**, 114010 (2012) doi:10.1103/PhysRevD.86.114010 [arXiv:1206.5500 [hep-ph]]; N. N. Achasov and A. V. Kiselev, Int. J. Mod. Phys. Conf. Ser. **35**, 1460447 (2014). doi:10.1142/S2010194514604475
- [43] L. Y. Dai and U. G. Meißner, arXiv:1706.10123 [hep-ph]. Some related earlier works are in L. Y. Dai, X. G. Wang and H. Q. Zheng, Commun. Theor. Phys. **57**, 841 (2012) doi:10.1088/0253-6102/57/5/15 [arXiv:1108.1451 [hep-ph]] and L. Y. Dai, X. G. Wang and H. Q. Zheng, Commun. Theor. Phys. **58**, 410 (2012) doi:10.1088/0253-6102/58/3/15 [arXiv:1206.5481 [hep-ph]].
- [44] N. N. Achasov, Phys. Atom. Nucl. **65**, 546 (2002) [Yad. Fiz. **65**, 573 (2002)]. doi:10.1134/1.1465495
- [45] The Review “Note on scalar mesons below 2 GeV” in Ref. [27].
- [46] F. E. Close and N. A. Tornqvist, J. Phys. G **28**, R249 (2002) doi:10.1088/0954-3899/28/10/201 [hep-ph/0204205].
- [47] H. W. Ke, X. Q. Li and Z. T. Wei, Phys. Rev. D **80**, 074030 (2009) doi:10.1103/PhysRevD.80.074030 [arXiv:0907.5465 [hep-ph]].